

## Raman Spectroscopic Studies of THF Clathrate Hydrate

C. A. Tulk,\* D. D. Klug, and J. A. Ripmeester

Steacie Institute for Molecular Sciences, National Research Council of Canada, Ottawa, Canada K1A 0R6

Received: March 16, 1998; In Final Form: June 9, 1998

Raman spectra were collected for tetrahydrofuran (THF) hydrate, a structure II clathrate hydrate (CH) that was prepared from THF and a dilute solution of D<sub>2</sub>O in H<sub>2</sub>O (5% D<sub>2</sub>O) in a 17:1 ratio. The vibrational modes observed include (1) the uncoupled O–D vibrational modes of HDO in H<sub>2</sub>O between 10 and 170 K and (2) the THF ring breathing mode (predominantly C–C–C–C stretches) between 10 and 170 K. The low-frequency host lattice modes and the THF C–H stretching modes at 10 K are also presented. The spectral line attributed to the C–C–C–C vibrational mode of the enclathrated THF molecules broadened, and a pronounced shoulder developed on the low-frequency side as the temperature decreased. This anomalous behavior is attributed to the inhibition of rapid reorientational motion of the enclathrated THF molecules at  $T < 100$  K. Analysis of the uncoupled O–D vibrations indicates that the frequency increases (and thus the hydrogen bond strength decreases) with increasing temperature. The vibrational frequency of the uncoupled O–D oscillator in hydrogen-bonded systems is sensitive to the hydrogen-bonded O–H–O length, and thus the highest density of hydrogen bond length in THF structure II clathrate was found to be 2.766 and 2.778 Å at 10 and 170 K, respectively. The distribution of hydrogen bond lengths is also briefly discussed.

### Introduction

Clathrate hydrates (CH's) are a class of inclusion compounds in which small molecules, known as guests, occupy cages in a lattice formed by water molecules, known as the host. Naturally occurring CH's, found in the arctic permafrost and offshore on the continental margins, are thought to contain vast amounts of hydrocarbon gases and as a result have recently been the subject of intense technical and scientific study.<sup>1</sup> There are three CH structures for which a large number of guests are known: structure I which is crystallographically cubic, space group  $Pm\bar{3}n$ , contains 46 water molecules per unit cell with  $a \sim 12$  Å; structure II, which is also crystallographically cubic, space group  $Fd\bar{3}m$ , contains 136 water molecules per unit cell with  $a \sim 17$  Å; and, structure H which is crystallographically hexagonal, space group  $P6/mmm$ , contains 34 water molecules per unit cell with  $a \sim 12$  Å and  $b \sim 10$  Å. For an excellent review of the structural properties and range of guest molecules of CH's, see ref 2.

Tetrahydrofuran forms a structure II CH (ideal composition THF·17 H<sub>2</sub>O) with the THF molecules held in the large 16-hedral cage<sup>3</sup> and interacting with the water molecules through weak interactions.<sup>4</sup> It is known from NMR studies that the THF molecules undergo rapid reorientational motion at 200 K and that this motion becomes slow on an NMR time scale below 30 K.<sup>5,6</sup> Calorimetric studies, conducted from 17 to 261 K,<sup>7</sup> have shown that when the heat capacity of the empty hydrate lattice (modeled using the ice Ih structure) was subtracted from the measured heat capacity, the heat capacity of the guest THF molecule could be obtained. This gave a barrier to rotation of the THF molecule at low temperatures of 3.5 kJ/mol. The activation energy for reorientation has also been calculated from NMR and dielectric relaxation data and found to be 3.84 kJ/mol for the enclathrated THF molecules and 30.1 kJ/mol for the host water molecules.<sup>5</sup> The corresponding activation energy for pure ice Ih is 55.2 kJ/mol, indicating that at any given temperature the reorientation of water molecules in the clathrate

structure is considerably faster than in pure ice.<sup>8</sup> Both NMR and dielectric studies also require that the reorientation of the encaged THF molecules at low temperatures has a very broad distribution of reorientation times.<sup>9</sup> The characteristic THF guest molecule reorientation time was calculated to be  $1.5 \times 10^{-8}$  s at 43 K from the dielectric data.<sup>5</sup> Recently, neutron diffraction studies on CH samples partially ordered by KOH doping indicate that at low temperatures the THF molecules have preferred orientations and that the low-temperature phase exhibits local lattice distortion leading to a quasi-tetragonal structure.<sup>10</sup> In the same paper it was suggested that at low temperatures the THF molecules assume preferred orientations, with the oxygen atoms pointing in the [001] direction and the molecular plane coinciding with the (110) mirror plane of the cage. However, the authors conclude that a distribution among nearly equivalent sites may be possible, thus indicating that the potential minima likely are very shallow. Far-IR studies of THF CH have investigated the low-frequency librational motion of enclathrated THF molecules<sup>4</sup> and have reported two broad bands centered at 25 and 38 cm<sup>-1</sup>. These bands result from oscillations about the two principal axes perpendicular to the THF molecular dipole axis, and the breadth of the bands, even at very low temperature, was attributed to a variation in force constants from cage to cage due to the disordered nature of the host water molecules.<sup>4</sup> Additional infrared spectroscopic studies have also been performed on thin films of pure THF CH's made from amorphous vapor deposited THF and water.<sup>11</sup> Infrared absorption attributed to crystalline THF CH's was noted to be in the region of 1073 cm<sup>-1</sup> and was assigned to a C–O–C stretching vibration of the THF molecule. This band was shown to form a distinct shoulder at low temperature due to a distribution of static THF molecular orientations over inequivalent positions in the large CH cage.<sup>12</sup> More recently, a detailed analysis of the infrared gas-phase spectra of pure THF indicates that the very strong line centered on 1087.8 cm<sup>-1</sup> is predominantly due to an asymmetric stretch of the COC bond.<sup>13</sup>

The Raman spectra of THF CH's have been investigated at temperatures between 250 and 275 K.<sup>14,15</sup> Spectra were recorded in the frequency ranges 100–350, 2200–2800, and 2800–3500  $\text{cm}^{-1}$ . (It should be noted however that the detailed nature of the vibrational spectra of  $\text{H}_2\text{O}$  ice above 3000  $\text{cm}^{-1}$ , and  $\text{D}_2\text{O}$  ice above 2200  $\text{cm}^{-1}$ , has been the subject of study and much controversy for many years.<sup>16</sup> The problem was investigated by Whalley,<sup>17</sup> who suggested that the broad Raman-active modes arise from the coupled oscillator motion of the O–H vibrations and the low-frequency, most intense Raman-active mode centered at 3083  $\text{cm}^{-1}$  arises from the in-phase symmetric stretching motion. The spectrum of an isolated O–D, or O–H, vibration can be studied by mixing a dilute solution (<5%) of  $\text{D}_2\text{O}$  in  $\text{H}_2\text{O}$ , or  $\text{H}_2\text{O}$  in  $\text{D}_2\text{O}$ .<sup>18</sup> More recently, the subject has been studied using MD simulations using the NCC potential function which calculated that the symmetric and antisymmetric peaks for  $\text{D}_2\text{O}$  ice Ih were located at 2550 and 2670  $\text{cm}^{-1}$  respectively.<sup>19,20</sup>) The lattice modes, 100–350  $\text{cm}^{-1}$ , were found to be similar to those in ice Ih, the only difference being that the Raman spectra of the clathrate lattice modes were somewhat broader. The coupled O–H (O–D) vibrational frequencies, 2800–3500  $\text{cm}^{-1}$  (2200–2800  $\text{cm}^{-1}$ ), were found to decrease with increasing pressure and decreasing temperature. An attempt was made to use the frequencies of coupled O–H, and O–D, vibrations to infer information on the hydrogen bond strength and structure.<sup>14</sup> To our knowledge, a detailed study of the CH's uncoupled O–D oscillator in a dilute solution of  $\text{D}_2\text{O}$  in  $\text{H}_2\text{O}$  has not been carried out.

A detailed knowledge of the vibrational modes of the guest molecules, the host molecules, and the host lattice is necessary for complete analysis of the dynamic and thermal properties of the CH system. In this paper, the Raman spectra due to vibrations of the host water molecules and the guest THF molecules between 10 and 170 K are reported. The CH water lattice modes are compared with those in ice Ih,<sup>21</sup> and the THF C–H stretching band is compared with that of solid THF. The Raman spectra of the ring breathing mode<sup>13</sup> (i.e., stretching modes of the C–C–C–C frame,  $\nu_{13}$  in the mid-IR) of enclathrated THF molecules are also presented for the temperature range between 10 and 170 K. This band, like the asymmetric COC stretch, broadens with decreasing temperature, a feature that is attributed to THF molecules distributed among inequivalent sites in the larger structure II cage. Data for uncoupled O–D oscillators are reported and used to characterize the distribution of hydrogen bond lengths in structure II clathrates.

## Experimental Section

Polycrystalline samples (~20 mL) of THF CH's were made by mixing THF (Fisher Scientific, 99.9%) and distilled water containing 5%  $\text{D}_2\text{O}$  in a molecular ratio of 1:17. The solution was placed in a test tube along with a small, 4 mm  $\times$  4 mm  $\times$  6 mm, copper U-shaped sample containment channel. (U-shaped sample channels were used so that the laser beam could enter the opened end of the channel and light scattered at 90° could be collected out the side.) The temperature was reduced to approximately  $-10^\circ\text{C}$ . The solution subsequently froze directly into the U-shaped channels, resulting in a fine-grained polycrystalline specimen that contained many microscopic cracks. To improve the optical quality of the sample, the temperature was held constant at  $T = -10^\circ\text{C}$  for approximately 5 h, to allow complete freezing, before being raised to  $T = 0^\circ\text{C}$  for approximately five more hours. This annealing process

resulted in a significant improvement in the transparency of the sample. Using a spring-loaded clip, the U-shaped channel containing the sample was held flat against a cooled ( $-15^\circ\text{C}$ ) copper sample holder, which was designed to be easily mounted on a Displex cryotip (Air Products, model DE-202).

Dry ice was used to transport the sample from the freezer to the Displex in a  $\text{CO}_2$  atmosphere. The temperature of the sample was measured using a gold–iron thermocouple attached to the Displex cryotip, which was equipped with a programmable temperature controller capable of maintaining a preset temperature within  $\pm 2$  K. After removing the vacuum shroud, the Displex cryotip was cooled to 270 K, after which the copper sample holder was quickly attached and the vacuum shroud replaced. From 270 K the sample was cooled at 5 K/min to 200 K, to reduce the amount lost due to sublimation, and then further cooled at 1 K/min to 10 K, to minimize the formation of microscopic cracks and prevent loss of optical quality. Any atmospheric water that condensed onto the sample during the transfer from the  $\text{CO}_2$  atmosphere to the Displex cryotip sublimed away immediately after the vacuum was applied.

Monochromatic laser light of 514.5 nm and approximately 150 mW from a Coherent Innova 90-4 argon ion laser was passed through an Applied Physics monochromator to eliminate the argon plasma lines and focused onto the sample with a 10 cm focal length lens. The laser light was depolarized due to multiple reflections within the sample, and the light scattered at 90° was collected with an  $f/1.8$  (50 mm focal length) lens and focused through a polarization scrambler onto the entrance slits of a SPEX model 1403 double monochromator. (No further polarization analysis was performed.) All spectra in this experiment were collected in this manner. The step size between datum points was set to 0.2  $\text{cm}^{-1}$ , and an integration time of 3.0–4.0 s was used. The monochromator was calibrated with mercury emission lines, and the resolution was 2  $\text{cm}^{-1}$  at 3200  $\text{cm}^{-1}$  with the entrance slits set to 200  $\mu\text{m}$ . Light that passed through the spectrometer was detected with a Hitachi photomultiplier (PM) tube operating in photon counting mode, and the output was passed through a discriminator before being saved with a computerized data acquisition system.

## Guest Molecular Modes

Raman spectra of the intramolecular vibrational modes between 850 and 975  $\text{cm}^{-1}$  of enclathrated THF in the temperatures range  $T = 10$ –170 K are shown in Figure 1. These spectra were collected from the same sample volume and for comparison purposes have been normalized and plotted against arbitrary intensity units. A detailed normal-coordinate analysis by Cadioli et al.<sup>13</sup> has shown this band to be predominantly due to C–C–C–C stretching vibrations with only a very weak contribution from C–H rocking motion. This mode can therefore be thought of as a ring-breathing mode and appears as a very strong line centered at 913  $\text{cm}^{-1}$  in the Raman spectrum of liquid THF at room temperature. The weak line at 890.8  $\text{cm}^{-1}$  is thought to be due to symmetric C–O–C stretching vibrations.

The most striking feature of the enclathrated THF ring breathing mode is the behavior below  $T = 100$  K and is revealed in this Raman band as a pronounced shoulder on its low-frequency side. This behavior is attributed to the THF molecules assuming a distribution over inequivalent potential minima in the CH's structure II large cage at low temperature (as was noted before for the asymmetric C–O–C stretch in the infrared<sup>12</sup> spectrum of the vibrational mode centered at 1073  $\text{cm}^{-1}$ ). At higher temperatures the Raman spectra become more symmetric;

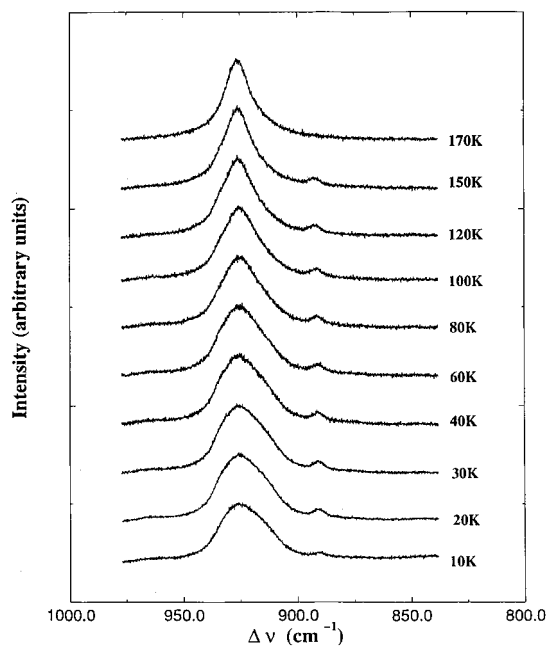


**Figure 1.** Raman spectra (see Experimental Section for scattering geometry) resulting from the ring breathing modes (predominantly C–C–C–C stretching modes) of enclathrated THF molecules at various temperatures. The weak peak centered on  $890.7 \text{ cm}^{-1}$  results from the C–O–C symmetric stretch. The sample optical quality had deteriorated at  $T = 170 \text{ K}$  due to sublimation, and the line at  $890.7 \text{ cm}^{-1}$  could not be observed.

the intensity of the low-frequency shoulder steadily decreases as  $T$  is raised, indicating that the distribution of vibrational modes, resulting from a distribution of THF molecular orientations, has narrowed. It seems likely that this is due to thermally activated reorientational motion of the guest molecules on the time scale of the molecular breathing vibrations. At  $T = 100 \text{ K}$  the shoulder has disappeared, resulting in a somewhat symmetric line shape, and at  $T = 120 \text{ K}$  the line shape can, to a good approximation, be represented by a Lorentzian function with a small Gaussian contribution; however, there is a slight distortion on the high-wavenumber side. The position of the Raman band does not depend on temperature; the difference between the half-height and the band maximum is plotted as a function of temperature in Figure 2. Differences between the half-height at half-maximum and the band maximum corresponding to the low- and high-frequency shift side are given by “□” and “○”, respectively. It is clear from this figure that at temperatures below  $80 \text{ K}$  the Raman band shape is very asymmetric, and the band does not become symmetric until the temperature reaches at least  $100 \text{ K}$ . The width of the band decreases steadily as the temperature is raised above  $100 \text{ K}$ .

These data indicate that the effects of hindered molecular reorientational motion can be observed at relatively high temperatures ( $120 \text{ K}$  and below). However, NMR data<sup>5,6</sup> suggest that large-amplitude reorientational motion is already present at  $30 \text{ K}$ . These two seemingly opposing views are consistent when we consider the characteristic time scale for the two techniques. The THF molecules jump between potential minima at low rates ( $\sim 10^{-5}$ – $10^{-6} \text{ s}$ ) at  $30 \text{ K}$ , thus exhibiting motional averaging on an NMR time scale. This is much slower than the time scale of molecular vibration so that Raman data result from each inequivalent state. At higher temperatures THF molecules exhibit faster reorientational motion that, in effect, averages the potential states, resulting in a symmetric Raman spectrum. Note that with an activation energy of  $3.84 \text{ kJ/mol}$ , obtained from relaxation time data, the THF reorientation time

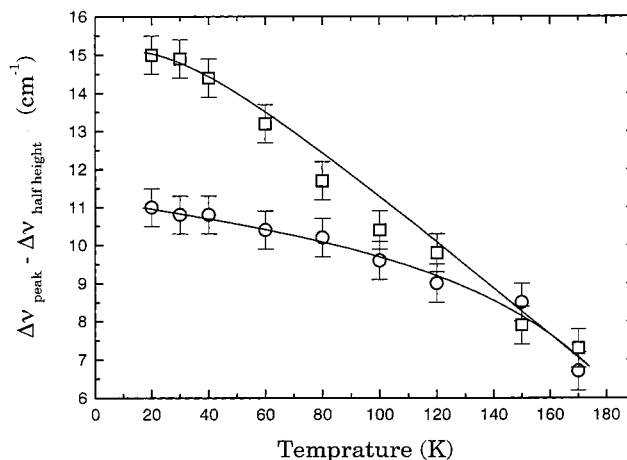


**Figure 2.** Plot of the difference in the Raman band maxima,  $\Delta\nu_{\text{peak}}$ , and the Raman band half-height,  $\Delta\nu_{\text{half-height}}$ . The low-frequency side is indicated by □, and the high-frequency side is indicated by ○; the errors shown represent the uncertainty in determining the band center and the band half-height. The solid lines are drawn to aid the eye. When the datum points coincide (within experimental error), the peak can be thought of as symmetric; this occurs at  $T = 100 \text{ K}$ . The band half-width continues to decrease as the temperature increases above  $100 \text{ K}$ .

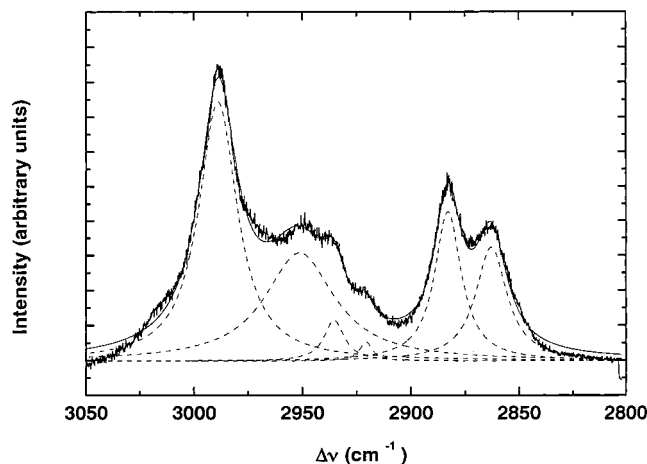


**Figure 3.** Raman spectrum (see Experimental Section for scattering geometry) of the C–H vibrational modes of the enclathrated THF molecule,  $2800 \text{ cm}^{-1} < \Delta\nu < 3030 \text{ cm}^{-1}$ . The spectrum of the coupled O–H water vibrations of the host lattice are above  $3030 \text{ cm}^{-1}$ , and the low-frequency tail of this band has been subtracted from this figure. The dashed lines represent Lorentzian functions fitted for the purpose of finding peak positions. (The second derivative of the Raman spectrum (smoothed) and the fitted curve representing the spectrum were found to agree, thus the band centers indicated by the fitted Lorentzian distributions are considered to accurately represent the band centers of each C–H mode.)

is  $\sim 8 \times 10^{-6} \text{ s}$  at  $30 \text{ K}$  and  $\sim 7 \times 10^{-11} \text{ s}$  at  $120 \text{ K}$ , assuming a simple exponential Arrhenius behavior. However, at  $120 \text{ K}$  the reorientational rate is close to that for a free molecule in a low-pressure gas (calculated from simple moment of inertia analysis to be  $\sim 3 \times 10^{-11} \text{ s}$ ); the molecule could be almost freely rotating in the cage. These values are compared with the ring-breathing (C–C–C–C stretch) vibrational period of  $\sim 3.6 \times 10^{-14} \text{ s}$ .

Raman spectra of the molecular C–H stretching vibrations of enclathrated THF molecules at  $10 \text{ K}$  are shown in Figure 3, and similar spectra for crystalline THF (c-THF) at  $100 \text{ K}$  have also been collected. The dashed lines of Figure 3 represent Lorentzian functions fitted for the purpose of determining the band centers. Assignments of these vibrational modes were made on the basis of normal-mode analysis of c-THF at  $85 \text{ K}$ ,<sup>13</sup>

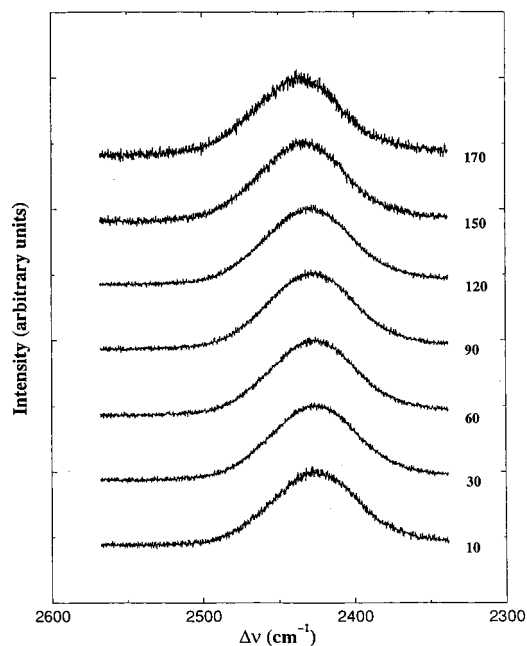


**Figure 4.** Raman spectra (see Experimental Section for scattering geometry) of the isolated O–D modes of the water molecules making up the host lattice. The temperature is given on the right in kelvin. The frequency shift,  $\Delta\nu$ , increases as the temperature increases above 90 K. The optical quality of the sample has deteriorated at  $T = 170$  K due to sublimation.

**TABLE 1: C–H Vibrational Frequencies ( $\text{cm}^{-1}$ )**

enclathrated	solid THF	assignment <sup>a</sup>
2863	2860	$\nu_{21}$ , CH <sub>2</sub> symmetric stretch, CH <sub>2</sub> asymmetric stretch
2883	2879	$\nu_4$ , CH <sub>2</sub> symmetric stretch, CH <sub>2</sub> asymmetric stretch
2920	2924	$\nu_3$ , CH <sub>2</sub> symmetric stretch, CH <sub>2</sub> asymmetric stretch
2935	2939	$\nu_{19}$ , CH <sub>2</sub> symmetric stretch, CH <sub>2</sub> asymmetric stretch
2950	2950	$\nu_2$ , CH <sub>2</sub> symmetric stretch, CH <sub>2</sub> asymmetric stretch
2989	2990	$\nu_{18}$ , CH <sub>2</sub> asymmetric stretch

<sup>a</sup> See ref 13.

and by comparison, the assignments for enclathrated THF molecules are presented in Table 1. (The values quoted for c-THF are those measured in the present study.) The tail of the Raman band of the coupled O–H vibrations (above 3025  $\text{cm}^{-1}$ ) of the host lattice molecules has been subtracted from the spectrum shown in Figure 3. It is known that the low-frequency mode, centered on 3084  $\text{cm}^{-1}$ , is predominantly of symmetric character.<sup>16,17</sup> A detailed discussion of the host molecular modes from uncoupled oscillator data is given in the next section.

### Host Vibrational Modes

The Raman spectra of the uncoupled O–D vibrational modes in a 5% solution of D<sub>2</sub>O in H<sub>2</sub>O are shown in Figure 4. (All of the spectra presented have been collected from the same scattering volume and for comparison have been normalized and plotted against arbitrary intensity units.) The vibrational frequency increases with temperature between 10 and 170 K, and the full width at half-maximum (fwhm) does not change significantly with temperature; the average fwhm over this temperature range is  $67.1 \pm 1.0 \text{ cm}^{-1}$ . Data were not collected above 170 K due to rapid sublimation of the sample that resulted in significant deterioration of its optical quality.

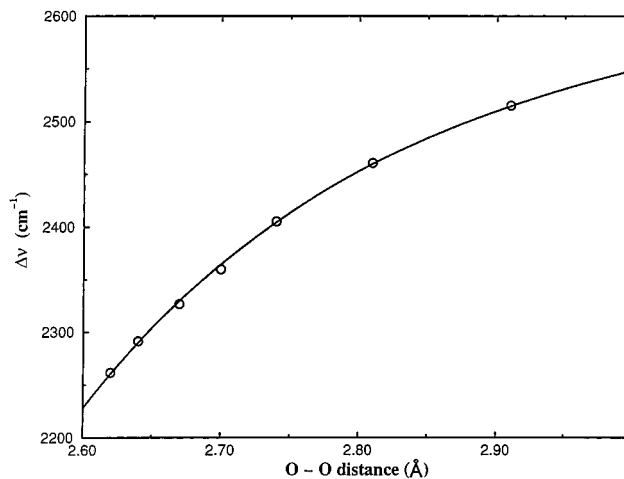


**Figure 5.** Hydrogen-bonded O–H...O distance as a function of the isolated O–D vibrational frequency. The open circles represent data collected from the X-ray analysis of D<sub>2</sub>O ice VII and infrared spectra of the vibrational modes. The solid line has been fitted using the parameters quoted in eq 1.

It is well-known that Raman spectra of decoupled O–H, or O–D, oscillators in D<sub>2</sub>O, or H<sub>2</sub>O, respectively, depend strongly on the hydrogen-bonded O–H...O length. This means that the O–H...O length can be related to the frequency of the localized oscillator. A number of correlations between the frequency of the O–H or O–D oscillator and the O–H...O or O–D...O bond length have been presented in the literature.<sup>16,25</sup> Although the dominant parameter in the determination of the frequency is the hydrogen bond length, other factors such as proton disorder and distribution of OOO bond angles about the tetrahedral positions (departure of OOO angle from tetrahedral in the average CH structure II<sup>22</sup> is 2.79°) are also expected to contribute, but to a lesser degree. The Raman intensities are dependent on the first derivative of the molecular polarizability with respect to normal vibrational coordinates, and it has been argued that the mean polarizability of a water molecule in ice changes with OH distance at a rate of approximately 0.5 Å<sup>2</sup>.<sup>28</sup> Therefore, the relative intensity of the Raman band varies only slightly over the hydrogen bond length of interest in this study. The Raman frequency shifts, and peak half-widths, can to a good approximation be converted into an O–H...O hydrogen bond distance through known correlations. This information can provide further insight into the local hydrogen-bonding structure of the THF clathrate.

One particularly useful correlation between the O–H frequency and the O–H...O distance was made using the infrared spectrum of uncoupled O–H frequencies and X-ray diffraction data for D<sub>2</sub>O ice VII at 22 °C between 0 and 189 bar.<sup>23,24</sup> These data correlate a wide range of hydrogen-bonded O–H...O distances, with vibrational frequencies. The ratio of the O–D to O–H vibrational frequencies is  $1.353 \pm 0.001$ . A plot of the vibrational frequency of the uncoupled O–D vibration versus the O–H...O hydrogen bond length from this correlation is shown in Figure 5. The analytical representation of this correlation is

$$\nu_{\text{OD}} = 2782.1 - 1560.1 \exp(-R/1.474) - 269351.6 \exp(-(R/0.9938)^2)$$

where  $R$  is the O–H...O bond length and is also plotted in Figure 5. The O–D frequency for an isolated water molecule is 2782.1  $\text{cm}^{-1}$ . The data plotted in Figure 5 and the above equation were used to estimate the distribution of hydrogen-

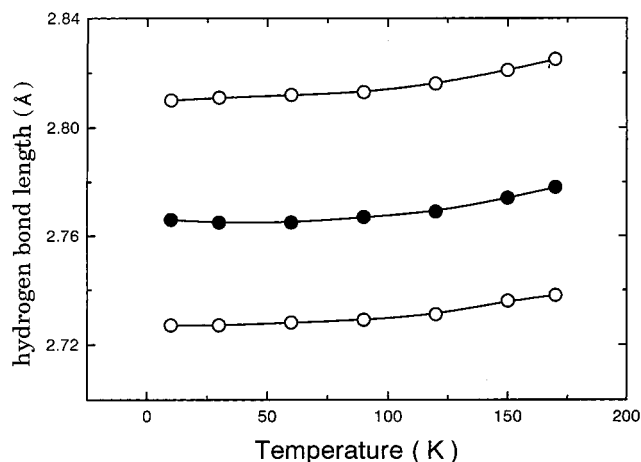


**Figure 6.** Approximate hydrogen bond length as a function of temperature. The O—H—O distance, estimated using eq 1 and the Raman shift, is indicated by ●, and the distribution of the O—H—O distance, estimated using eq 1 and the frequency at the band half-heights, is indicated by ○. The length distribution of hydrogen bonds in clathrate hydrates ( $0.05 \pm 0.005$  Å) is significantly larger than that of pure crystalline ice ( $0.03 \pm 0.005$  Å).

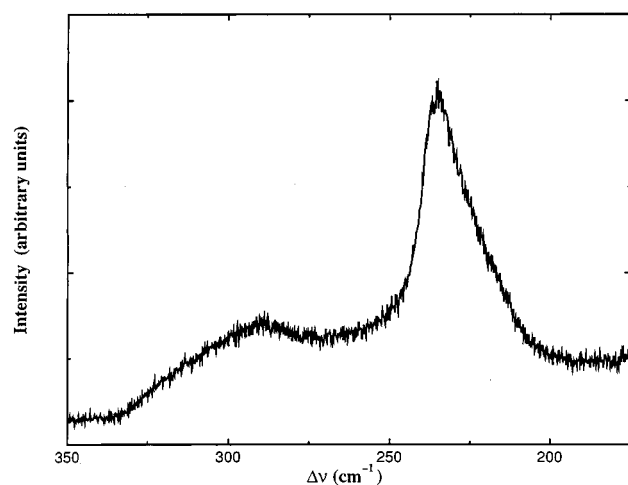


**Figure 7.** Raman spectrum (see Experimental Section for scattering geometry) of the low-frequency lattice vibrational modes of THF clathrate hydrates at 10 K. Spectra at higher temperature were not collected due to the optical quality of the sample and specularly reflected incident laser light.

bonded O—H—O distances. The relation used indicates a frequency shift of  $875 \text{ cm}^{-1}/\text{Å}$ , in reasonable agreement with other the experimental and theoretical correlations in the literature. The frequency shift with O—D—O distance is about  $800 \text{ cm}^{-1}/\text{D}$  as determined from a series of ice phases and clathrate hydrates,<sup>25</sup> and a theoretical analysis based on a quantum calculation for ice lattices gives about  $833 \text{ cm}^{-1}/\text{Å}$ .<sup>26</sup>

Figure 6 shows (1) the O—H—O distance estimated from eq 1 and the Raman frequency shift,  $\Delta\nu_{\text{peak}}$ , and (2) the distribution of the O—H—O distance estimated from eq 1 and the frequency at half the height of the band,  $\Delta\nu_{\text{half-height}}$ , as a function of temperature for the present data. The distribution of hydrogen bond lengths in the CH's structure II has been measured previously, and at higher temperatures four bond lengths were found, 2.767, 2.776, 2.796, and 2.812 Å.<sup>27</sup> The line width data shown in Figure 6 are in good agreement with these values.

Raman spectra in the region of water lattice modes of structure II THF CH's between 200 and  $330 \text{ cm}^{-1}$  are shown in Figure 7. The Raman spectra of the lattice modes of ice Ih at 10 K between 200 and  $350 \text{ cm}^{-1}$  bear a striking resemblance

to the spectra of the THF CH's in the same region, and the spectrum of ice Ih is characteristic of a disordered solid. This is in contrast to the spectra of the ordered high-pressure forms of pure ice where the spectra consist of a series of narrow bands. The Raman spectra of the lattice modes of ice Ih can be generally understood in terms of a minimum of two force constants representing O...O stretching and O—O—O bending force constants.<sup>21</sup> The strong low-frequency mode observed for the CH's is at  $235 \text{ cm}^{-1}$  with a very broad sloping low-frequency side and a very sharp high-frequency side. The fwhm of this peak is  $20 \text{ cm}^{-1}$  while the same peak in ice Ih is located at  $227 \text{ cm}^{-1}$  at  $T = 100 \text{ K}$  and has a fwhm of  $10 \text{ cm}^{-1}$ . The broad features of these clathrate hydrate Raman spectra result from the orientational disorder leading to a relaxation of selection rules. Another less intense peak occurs at  $289 \text{ cm}^{-1}$ .

## Summary and Conclusions

The reorientational motion of enclathrated THF molecules, which is restricted due to van der Waals interactions with the host water lattice, has been observed using Raman spectroscopy. The THF ring breathing mode, which is symmetric at high temperatures, broadens significantly and becomes asymmetric at low temperature. Rough activation energy analysis using data obtained from NMR and dielectric experiments suggests that the reorientational rate of enclathrated THF molecules approaches that of the isolated molecule at about 120 K. The rapid reorientational motion of the thermally activated THF molecules at 120 K results in a symmetric Raman line shape for the ring breathing band.

The bandwidths of the uncoupled OD vibrational spectra of the host water lattice between 10 and 170 K in the THF clathrate hydrate were used to characterize the distribution of O—H—O hydrogen bond lengths. They range from 2.727 to 2.810 Å at 10 K and from 2.738 to 2.825 Å at 170 K. These data are in good agreement with data collected at higher temperatures.

## References and Notes

- Holder, G. D.; Kamath, V. A.; Godbole, S. P. *Annu. Rev. Energy* **1984**, *9*, 427.
- Jeffrey, G. A. In *Comprehensive Supramolecular Chemistry*; Atwood, J. L., Davis, J. E. D., MacNicol, D. D., Vögtle, F., Eds.; Elsevier: New York, 1996; Vol. 6, p 757.
- Davidson, D. W. In *Water—A Comprehensive Treatise*; Franks, F., Ed.; Plenum Press: New York, 1973; Vol. 2, p 115.
- Klug, D. D.; Whalley, E. *Can. J. Chem.* **1973**, *51*, 4062.
- Garg, S. K.; Davidson, D. W.; Ripmeester, J. A. *J. Magn. Reson.* **1974**, *15*, 295.
- Davidson, D. W.; Garg, S. K.; Ripmeester, J. A. *J. Magn. Reson.* **1978**, *31*, 399.
- White, M. A.; Maclean, M. T. *J. Chem. Phys.* **1985**, *89*, 1380.
- Hawkins, R. E.; Davidson, D. W. *J. Phys. Chem.* **1966**, *70*, 1889.
- Gough, S. R.; Hawkins, R. E.; Morris, B.; Davidson, D. W. *J. Phys. Chem.* **1973**, *77*, 2969.
- Yamamuro, O.; Matsuo, T.; Suga, H.; David, W. I. F.; Ibberson, R. M.; Leadbetter, A. J. *Physica B* **1995**, *213*, 405.
- Richardson, H. H.; Wooldridge, P. J.; Devlin, J. P. *J. Chem. Phys.* **1985**, *83*, 4387.
- Fleyfel, F.; Devlin, J. P. *J. Phys. Chem.* **1991**, *95*, 3811.
- Cadioli, B.; Gallinella, E.; Coulombeau, C.; Jobic, H.; Berthier, G. *J. Phys. Chem.* **1993**, *97*, 7844.
- Johari, G. P.; Chew, H. A. M. *Nature* **1983**, *303*, 604.
- Johari, G. P.; Chew, H. A. M. *Philos. Mag. B* **1984**, *49*, 281.
- Sceats, M. G.; Rice, S. A. In *Water—A Comprehensive Treatise*; Franks, F., Ed.; Plenum Press: New York, 1982; Vol. 7, p 83.
- Whalley, E. *Can. J. Chem.* **1977**, *55*, 3429.
- Haas, C.; Hornig, D. F. *J. Chem. Phys.* **1960**, *32*, 1763.
- Sciortino, F.; Corongiu, G. *J. Chem. Phys.* **1993**, *98*, 5694.
- Sciortino, F.; Corongiu, G. In *Methods and Techniques in Computational Chemistry METECC-95*; Clementi, E., Corongiu, G., Eds.; STEF: Cagliari, 1995; p 47.

(21) Wong, P. T. T.; Klug, D. D.; Whalley, E. In *Physics and Chemistry of Ice*; Jones, S. J., Gold, L. W., Eds.; Royal Society of Canada: Ottawa, 1973; p 87.

(22) Davidson, D. W. In *Water—A Comprehensive Treatise*; Franks, F., Ed.; Plenum Press: New York, 1973; Vol. 2, p 115.

(23) Klug, D. D.; Whalley, E. *J. Chem. Phys.* **1984**, *81*, 1220.

(24) Munro, R. G.; Block, S.; Mauer, F.; Piermarini, G. *J. Appl. Phys.* **1982**, *53*, 6174.

(25) Whalley, E. In *The Hydrogen Bond*; Schuster, P., Zundel, G., Sandorfy, C., Eds.; North-Holland: Amsterdam, 1976; Vol. III, p 1425.

(26) Knuts, S.; Ojamäe, L.; Hermanssen, K. *J. Chem. Phys.* **1993**, *99*, 2917.

(27) Mak, T. C. W.; McMullan, R. K. *J. Chem. Phys.* **1965**, *42*, 2732.

(28) Klug, D. D.; Mishima, O.; Whalley, E. *J. Chem. Phys.* **1987**, *86*, 5323.